

Hard production of a Z boson plus heavy flavor jets at LHC and the intrinsic charm content of a proton

A. V. Lipatov,^{1,2} G. I. Lykasov,² M. A. Malyshev,¹ A. A. Prokhorov,^{2,3} and S. M. Turchikhin²

¹*Skobeltsyn Institute of Nuclear Physics, Lomonosov Moscow State University, 119991 Moscow, Russia*

²*Joint Institute for Nuclear Research, 141980 Dubna, Moscow region, Russia*

³*Faculty of Physics, Lomonosov Moscow State University, 119991 Moscow, Russia*



(Received 23 February 2018; published 18 June 2018)

The cross section of associated production of a Z boson with heavy flavor jets in pp collisions is calculated using the SHERPA Monte Carlo generator and the analytical combined QCD approach based on k_T factorization at small x and conventional collinear QCD at large x . A satisfactory description of the ATLAS and CMS data on the p_T spectra of Z bosons and c jets in the whole rapidity, y , region is shown. Searching for the intrinsic charm (IC) contribution in these processes, which could be visible at large $y > 1.5$, we study observables very sensitive to nonzero IC contributions and less affected by theoretical QCD scale uncertainties. One of such observables is the so-called double ratio, the ratio of the differential cross section of $Z + c$ production in the central region of $|y| < 1.5$ and in the forward region $1.5 < |y| < 2.5$, divided by the same ratio for $Z + b$ production. These observables could be more promising for the search of IC at LHC as compared to the observables considered earlier.

DOI: [10.1103/PhysRevD.97.114019](https://doi.org/10.1103/PhysRevD.97.114019)

I. INTRODUCTION

Many hard processes within the Standard Model and beyond, such as the production of heavy flavor jets and of the Higgs boson and other processes, are quite sensitive to the heavy quark content of the nucleon. Studying the latter plays an increasingly significant role in the physics program of LHC. Strange, charm, and beauty parton distribution functions (PDFs) are essential inputs for the calculation of observables for these processes within the perturbative QCD (pQCD). Global QCD analysis allows one to extract the PDFs from comparison of hard-scattering data and pQCD calculations.

Hard production of vector boson (V) accompanied by heavy flavor (HF)¹ jets in pp collisions at LHC energies can be considered as an additional tool to study the quark and gluon PDFs compared to the deep inelastic scattering of electrons on protons. In these processes, in the rapidity region $|y| < 2.5$, which corresponds to the kinematics of ATLAS and CMS experiments, one can study these PDFs not only at low parton momentum fractions $x < 0.1$ but also at larger x values [1]. Therefore, such $V + \text{HF}$

processes can give us new information on the PDFs at large $x > 0.1$, where the nontrivial proton structure (for example, the possible contribution of valencelike *intrinsic* heavy quark components) can be revealed [2–5].

Intense studies of an intrinsic charm (IC) signal in the production of vector (Z and W) bosons or prompt photons γ accompanied by heavy flavor jets in pp collisions at LHC energies were made in Refs. [1,6–9]. It was shown that the contribution of IC to the proton PDFs can be visible in the transverse momentum spectra of $\gamma/Z/W$ or c/b jets in the forward rapidity region of the ATLAS and CMS kinematics, $1.5 < |y| < 2.5$, at large $p_T > 100$ GeV. The shape of these p_T spectra depends significantly on the IC probability in the proton w_{IC} , while in the more central rapidity region $|y| < 1.5$, the IC signal may not be visible.

Up to now, there has been a long-standing debate about the w_{IC} value [9–12] (see also Ref. [1] and references therein). A first estimate of the intrinsic charm probability in the proton was carried out in Ref. [13] utilizing recent ATLAS data on the production of prompt photons accompanied by c jets at $\sqrt{s} = 8$ TeV [14]. It is shown [13] that to extract the IC probability from these ATLAS data we have to eliminate a large theoretical uncertainty due to the QCD scale. In this paper, we focus on looking for observables in $Z + \text{HF}$ production processes, which are sensitive to the IC contribution in the proton PDF and are less dependent on the QCD scale. In Ref. [8], it is shown that such observables could be the ratio of $\gamma/Z + c$ and $\gamma/Z + b$ production cross sections in the forward rapidity

¹Here and below, heavy flavor implies charm and beauty quarks.

Published by the American Physical Society under the terms of the [Creative Commons Attribution 4.0 International license](https://creativecommons.org/licenses/by/4.0/). Further distribution of this work must maintain attribution to the author(s) and the published article's title, journal citation, and DOI. Funded by SCOAP³.

region $1.5 < |y^Z| < 2.5$. Calculations [8] were performed applying the Monte Carlo (MC) generator MCFM [15] and k_T factorization of QCD.

In this paper, we investigate $Z + \text{HF}$ production processes at LHC energies within two approaches: the combined QCD approach, based on the k_T -factorization formalism [16–18] in the small- x domain and on conventional (collinear) QCD factorization at large x , and the SHERPA MC event generator [19]. Recently, the combined QCD approach was successfully applied to describe LHC data on associated $Z + b$ production at $\sqrt{s} = 7$ TeV [20]. The SHERPA MC generator, which includes initial- and final-state parton showering, is supposed to provide a realistic description of multiparticle final states allowing for HF jets from higher perturbative orders, such as gluon splitting into heavy quark pairs. SHERPA can also model the full chain of hadronization and decays of unstable particles, which should allow us a more accurate comparison to experimental measurements of HF jets than achieved in previous studies [7,8]. Validation of these approaches is performed using ATLAS and CMS data [21,22] on Z boson production accompanied by charm and beauty jets for center-of-mass energies $\sqrt{s} = 7$ and 8 TeV. One of the goals of this work is to study the influence of intrinsic charm on various kinematical distributions in these processes and to investigate the effects of initial- and final-state parton showers in the description of LHC data. We also focus on finding new observables that are sensitive to the IC content of a proton and that could help us reduce the QCD scale uncertainties.

In Sec. II, we present two theoretical approaches adopted in our calculations. The results and discussion are presented in Secs. III and IV is the Conclusion.

II. THEORETICAL APPROACHES TO ASSOCIATED $Z + \text{HF}$ PRODUCTION

To calculate the total and differential cross sections of associated $Z + \text{HF}$ production within the combined QCD approach, we strictly follow the scheme described earlier [20]. In this scheme, the leading contribution comes from the $\mathcal{O}(\alpha_s^2)$ off-shell gluon-gluon fusion subprocess $g^* + g^* \rightarrow Z + Q + \bar{Q}$ (where Q denotes the heavy quark), calculated in the k_T -factorization approach. The latter has certain technical advantages in the ease of including higher-order radiative corrections in the form of transverse momentum-dependent (TMD) parton distributions (see Refs. [23–25] for more information). To extend the consideration to the whole kinematic range, several subprocesses involving initial-state quarks, namely, flavor excitation $q + Q \rightarrow Z + Q + q$, quark-antiquark annihilation $q + \bar{q} \rightarrow Z + Q + \bar{Q}$, and quark-gluon scattering $q + g \rightarrow Z + q + Q\bar{Q}$, are taken into account using the collinear QCD factorization (in the tree-level approximation). The IC contribution is estimated using the $\mathcal{O}(\alpha_s)$ QCD Compton scattering $c + g^* \rightarrow Z + c$,

where the gluons are kept off shell but the incoming non-perturbative intrinsic charm quarks are treated as on-shell ones.² Thus, we rely on a combination of two techniques, with each of them being used for the kinematics in which it is more suitable³ (off-shell gluon-gluon fusion subprocesses at small x and quark-induced subprocesses at large x values). More details of the above calculations can be found in Ref. [20].

In contrast to earlier studies [7,8] of $Z + \text{HF}$ production within the MCFM routine (that performs calculation in the fixed order of pQCD), in the present paper, the SHERPA 2.2.1 [19] MC generator is applied. It uses matrix elements that are provided by the built-in generators AMEGIC++ [30] and COMIX [31]; OPENLOOPS [32] is used to introduce additional loop contributions into the next-to-leading-order (NLO) calculations. We use matrix elements calculated at NLO for up to two final partons and at the leading order (LO) for three and four partons. They are merged with the SHERPA parton showering [33] following the ME+PS@NLO prescription [34]. This is different from the study of $Z + c$ production carried out in Ref. [12], in which the matrix element was calculated in the LO and merged following the ME+PS@LO method [35]. The latter approach was also used in this study as a cross-check, with the LO matrix element allowing for up to four final partons. In both approaches, the five-flavor scheme (5FS), in which c and b quarks are considered as massless particles in the matrix element and massive in both the initial- and final-state parton showers, is used. The SHERPA can also model the full chain of hadronization and unstable particle decays for an accurate comparison with experimental measurements of HF jets.

III. RESULTS AND DISCUSSION

A. Comparison with the LHC data at $\sqrt{s} = 7$ and 8 TeV

In this section, we present comparisons of our calculations for $Z + \text{HF}$ production made with the SHERPA generator and within the combined QCD approach to the LHC Run 1 data, in order to verify the applicability of these approaches for further predictions. Following Refs. [1,6–9], we mainly concentrate on the transverse momentum distributions of Z bosons and/or HF jets, where the IC effects are expected to appear.⁴

²The perturbative charm contribution is already taken into account in the off-shell gluon-gluon fusion subprocess.

³An essential point of consideration [20] is using a numerical solution of the Catani-Ciafaloni-Fiorani-Marchesini (CCFM) evolution equation [26–28] to derive the TMD gluon density in a proton. The latter smoothly interpolates between the small- x BFKL gluon dynamics and high- x Dokshitzer-Gribov-Lipatov-Altarelli-Parisi (DGLAP) dynamics. Following Ref. [20], below, we take the latest JH'2013 parametrization [29], adopting the JH'2013 set-2 gluon as the default choice.

⁴Recent ATLAS and CMS experimental data on associated $Z + b$ production taken at $\sqrt{s} = 7$ TeV as functions of other kinematical variables within the framework of the combined QCD approach are considered in Ref. [20].

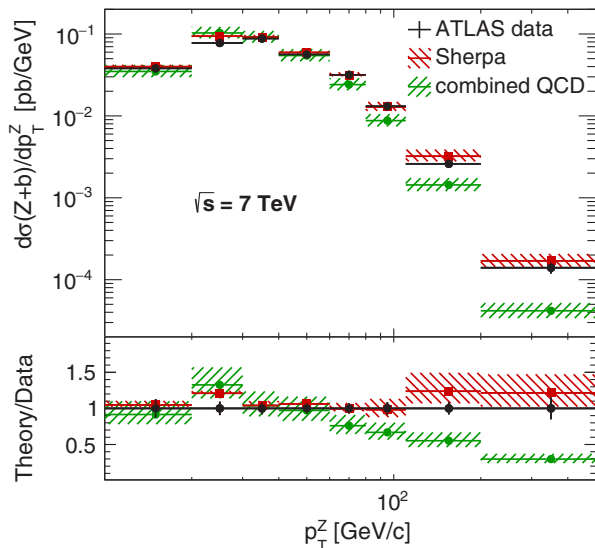


FIG. 1. Cross section of $Z + b$ -jet production as a function of the Z boson transverse momentum at $\sqrt{s} = 7$ TeV. The main panel shows the ATLAS measurement result [21] compared to SHERPA calculations and to combined QCD calculations. The uncertainty bands represent uncertainties in the QCD scale. The bottom panel shows the ratio of calculations to data.

The first comparison is performed for the associated $Z + b$ production cross section measured by the ATLAS Collaboration [21] at $\sqrt{s} = 7$ TeV. According to Ref. [21], the following selection criteria were applied to generated events. Two leptons originating from the Z boson decay are required to have an invariant mass $76 \text{ GeV} < m_{\ell\ell} < 106 \text{ GeV}$ with a minimum transverse momentum of each lepton $p_T^\ell > 20 \text{ GeV}$ and rapidity $|y^\ell| < 2.5$. In SHERPA-generated events, jets are built using all stable particles excluding the lepton pair from the Z boson decay with the anti- k_T algorithm with a size parameter $R = 0.4$. They are required to have a rapidity $|y^{\text{jet}}| < 2.4$ and minimum transverse momentum $p_T^{\text{jet}} > 20 \text{ GeV}$. Each jet is also required to be separated from any of the two leptons by $\Delta R_{\text{jet},\ell} > 0.5$. Jets are identified as b jets if there is a weakly decaying b hadron with a transverse momentum $p_T^b > 5 \text{ GeV}$ within a cone $\Delta R = 0.3$ around the jet direction. The same kinematic requirements are applied to final-state b quarks (treated as b jets at a parton level) when using the combined QCD approach. SHERPA results were obtained within the ME+PS@NLO model. In both approaches, the CTEQ66 PDF set [36] was used.

In Fig. 1, the associated $Z + b$ -jet production cross section (for events with at least one b jet) calculated as a function of the Z boson transverse momentum p_T^Z is presented in comparison with the ATLAS data [21]. Here and below, central values, marked by horizontal lines, correspond to the default choice of factorization and renormalization scales $\mu_R = \mu_F = m_T$, where m_T is the

Z boson transverse mass. Theoretical uncertainties of our calculations correspond to the maximum deviation between the nominal spectrum and those obtained by the usual factor 2 variations of renormalization and factorization scales.

One can see that the SHERPA results are in perfect agreement with the ATLAS data within the scale uncertainties in the whole p_T^Z range. In the combined QCD approach, we observe some underestimation of the data at high p_T^Z and a slight overestimation at low transverse momenta. The latter can be attributed to the TMD gluon density used in the calculations because the region $p_T^Z < 100 \text{ GeV}$ is fully dominated by the off-shell gluon-gluon fusion subprocess [20]. However, the results obtained within both approaches under consideration in this region are rather close to each other. A noticeable deviation of the combined QCD calculations from the data at large p_T^Z is explained by the absence of the effects of parton showers, hadronization, and additional contributions of NLO diagrams, including loop ones, in these calculations. Such contributions, which are taken into account by SHERPA, considerably improve the description of the data. The influence of the parton showers and of higher-order pQCD corrections is investigated in detail in the next section. It is important to note that our results obtained with SHERPA are in good agreement with the results obtained within a similar approach [37].

Now, we turn to the associated $Z + c$ -jet production measured by the CMS Collaboration at $\sqrt{s} = 8$ TeV [22]. The following selection criteria are applied to generated events for this comparison. Two leptons originating from a Z boson decay must have an invariant mass $71 \text{ GeV} < m_{\ell\ell} < 111 \text{ GeV}$, a minimum transverse momentum of $p_T^\ell > 20 \text{ GeV}$, and pseudorapidity $|\eta^\ell| < 2.1$. Jets built with the anti- k_T algorithm with a size parameter $R = 0.5$ are required to have $p_T^{\text{jet}} > 25 \text{ GeV}$ and $|\eta^{\text{jet}}| < 2.5$ and to be separated from the leptons by $\Delta R_{\text{jet},\ell} > 0.5$. b - and c -flavor identification criteria similar to those described above are used.

In Fig. 2, our results for the differential cross sections of associated $Z + c$ -jet production calculated as functions of the Z boson and c -jet transverse momenta are shown in comparison with the CMS data [22]. A comparison with the measured ratio of the cross sections $\sigma(Z + c)/\sigma(Z + b)$ is also presented. We find that the particle-level SHERPA calculations agree well with the data. The parton-level combined QCD calculations also describe the CMS data within the theoretical and experimental uncertainties (except at low $p_T^c < 40 \text{ GeV}$), although they tend to underestimate the SHERPA results. As in the case of associated $Z + b$ -jet production, we attribute the latter to the parton showering effects and additional NLO contributions, missing in the combined QCD calculations (to be precise, mainly in the tree-level quark-induced subprocesses, since the off-shell gluon-gluon fusion only gives a

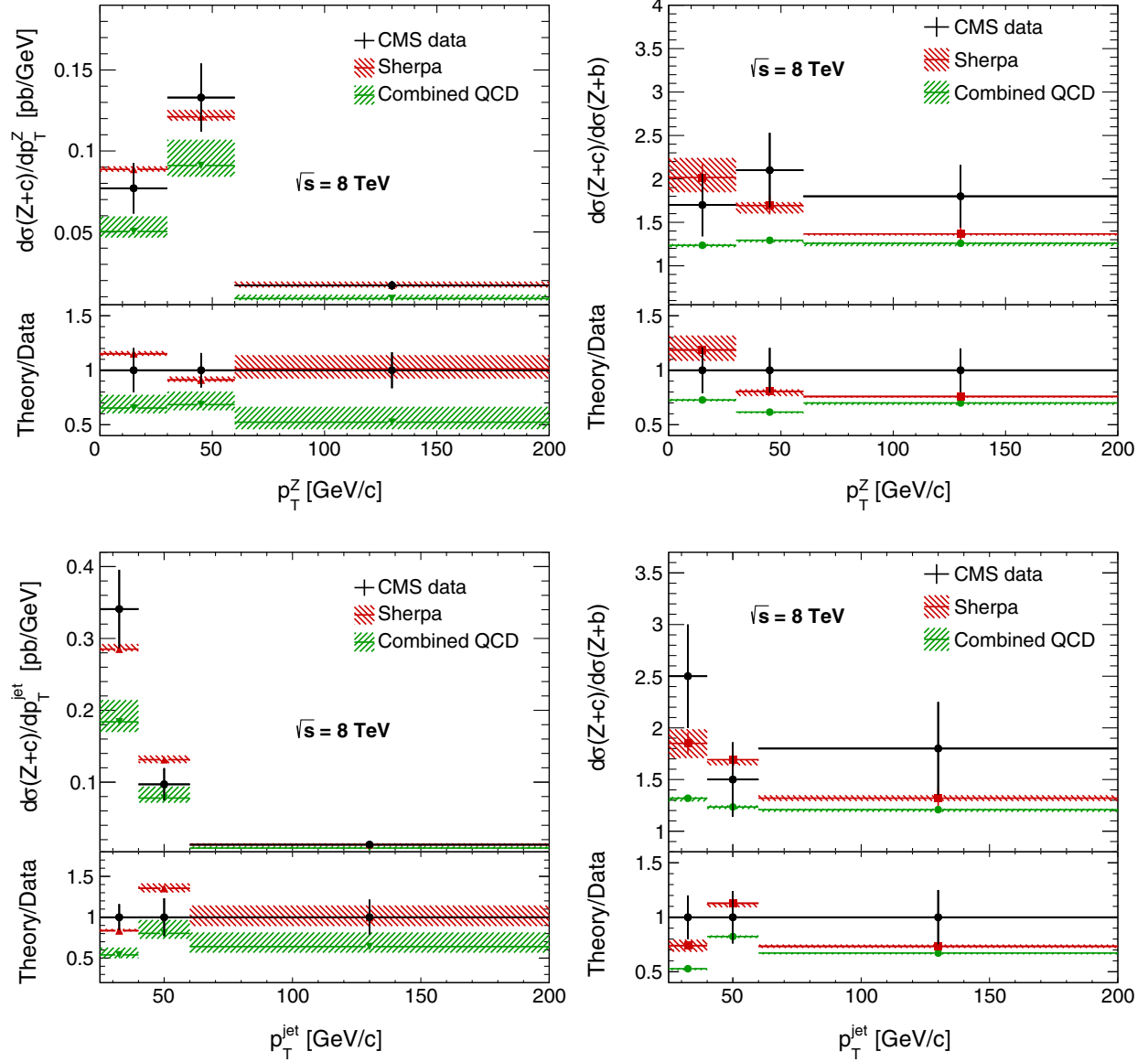


FIG. 2. Cross section of $Z + c$ -jet production (left) and the ratio of cross sections of $Z + c$ -jet and $Z + b$ -jet production (right) as a function of the Z boson (top) and HF-jet (bottom) transverse momenta at $\sqrt{s} = 8$ TeV. The main panels show the CMS measurement result [22] compared to the results of SHERPA and the combined QCD calculations. The uncertainty bands represent the uncertainties in the QCD scale. The bottom panels show the ratio of calculations to the data.

negligible contribution at large transverse momenta). Note that the scale uncertainties of our calculations partially cancel out when considering the $\sigma(Z + c)/\sigma(Z + b)$ ratio⁵ (see Fig. 2, right plots).

One can see that a better description of the CMS data is achieved with the SHERPA tool, and therefore we consider SHERPA calculations as the most reliable ones. Thus, we

⁵This ratio, being considered in the forward rapidity region $1.5 < y^Z < 2.5$, is sensitive to the IC content of a proton [8]. However, we checked that in the kinematical region probed by the CMS experiment [22] this IC dependence is negligible.

mainly concentrate on them when investigating the possible effects from IC in the LHC experiments below.

B. $Z + \text{HF}$ spectra for $\sqrt{s} = 13$ TeV and prediction for the IC contribution

The purpose of the calculation of $Z + \text{HF}$ differential cross sections in this paper is to investigate the effect of an IC signal on the observables, which can be measured at the LHC by general purpose detectors at $\sqrt{s} = 13$ TeV. As was mentioned above, a sensitivity to the IC at ATLAS and CMS experiments on $Z + c$ -jet production can be achieved in the forward rapidity region $1.5 < |y^Z| < 2.5$ and $p_T^Z > 50$ GeV [7,8]. In this kinematical region, the shape of the $\sigma(Z + c)/\sigma(Z + b)$

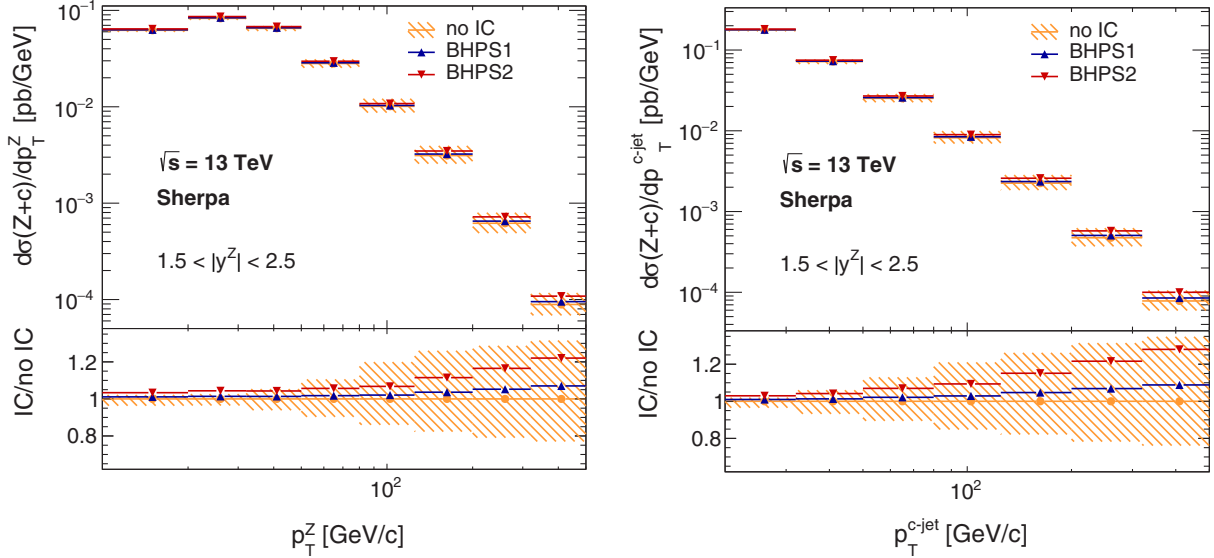


FIG. 3. Predictions for the cross section of $Z + c$ -jet production as a function of the Z boson (left) and c -jet (right) transverse momentum in the forward rapidity region $1.5 < |y^Z| < 2.5$ at $\sqrt{s} = 13$ TeV. The predictions are made with the SHERPA generator using the CT14NNLO PDF with different values for the IC contribution that correspond to BHPS1 and BHPS2 fits and without IC (no IC). The bottom panels show the ratio of predictions for nonzero values of IC to those for no IC. The uncertainty bands represent the uncertainties in the QCD scale (shown only for no IC predictions).

ratio is sensitive to effects of IC and is less affected by scale uncertainties than those of the transverse momentum spectra. This fact provides an opportunity to measure the IC contribution.

In SHERPA, predictions for $Z + \text{HF}$ production are calculated within the ME+PS@NLO model. They use the CT14NNLO PDF set [12] containing PDFs with Brodsky-Hoyer-Peterson-Sakai model [2,3] fits referred to as BHPS1 and BHPS2, corresponding to intrinsic charm momentum fraction $\langle x \rangle_{\text{IC}} = 0.6\%$ and $\langle x \rangle_{\text{IC}} = 2.1\%$, respectively [12]. The following selection criteria are used in this analysis. Two leptons from the Z boson decay are required to have a mass $76 \text{ GeV} < m_{\ell\ell} < 106 \text{ GeV}$, transverse momentum $p_T^\ell > 27 \text{ GeV}$, and rapidity $|y^\ell| < 2.5$. Jets are reconstructed from all stable particles, excluding the leptons, with the anti- k_T algorithm with parameters $R = 0.4$, and are required to have $|y^{\text{jet}}| < 2.5$ and $p_T^{\text{jet}} > 20 \text{ GeV}$, $\Delta R_{\text{jet},\ell} > 0.4$. The identification of heavy flavor jets is performed as follows. If there is a weakly decaying b hadron with $p_T^b > 5 \text{ GeV}$ within a cone of $\Delta R = 0.4$ around the jet direction, the jet is identified as a b jet. If it is not identified as such, the same criteria are applied for c hadrons, and the jet is identified as a c jet, if one is found.

In Fig. 3, differential cross sections of associated $Z + c$ -jet production calculated in the forward rapidity region $1.5 < |y^Z| < 2.5$ at $\sqrt{s} = 13$ TeV as functions of the c -jet and Z boson transverse momenta are shown. The effect of IC becomes visible at $p_T \gtrsim 200 \text{ GeV}$ in both distributions, but the theoretical uncertainties are still higher than the size of this effect in the whole transverse momentum region studied. However, in the ratios of differential cross sections $\sigma(Z + c)/\sigma(Z + b)$, the effect of IC can be visible at

significantly lower Z boson or HF-jet transverse momenta than in the differential cross sections themselves. Predictions for these ratios are shown in Fig. 4.

To investigate the influence of parton showers and higher-order pQCD corrections on the predictions, we repeated the above SHERPA calculations at a parton level using LO and NLO matrix elements. The results of these calculations are shown in Fig. 5 in comparison with the combined QCD predictions. First, one can see that the best agreement with the combined QCD approach at large transverse momenta is given by the SHERPA calculations using the LO matrix element. This is not surprising because the combined QCD predictions are represented in this kinematical region by the quark-induced subprocesses calculated in the usual collinear QCD factorization with the same accuracy. At low and moderate transverse momenta, the results of the combined QCD approach are consistently close to parton-level SHERPA predictions obtained at the NLO level, which demonstrates it is effective to take into account higher-order pQCD corrections in the off-shell gluon-gluon fusion subprocess supplemented with the CCFM gluon dynamics. Therefore, we can conclude that there are no large contradictions between our two theoretical approaches at the parton level. The combined QCD approach can be used to predict $Z + \text{HF}$ production cross sections at the parton level at moderate transverse momenta, but such approximation becomes worse toward high transverse momenta where the effects described above are quite large.

Next, the effects of adding parton showers and NLO corrections to the parton-level SHERPA LO predictions for differential cross section ratios $\sigma(Z + c)/\sigma(Z + b)$ are

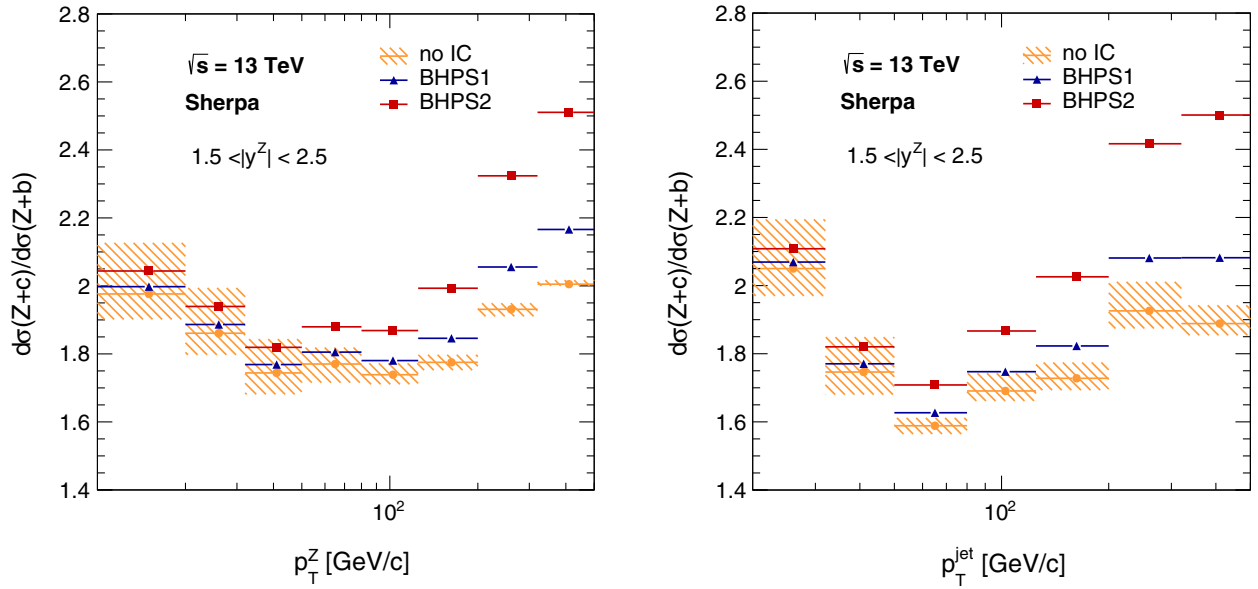


FIG. 4. Predictions for the ratio of $Z + c$ -jet and $Z + b$ -jet production cross sections as a function of the Z boson (left) and HF-jet (right) transverse momenta in the forward rapidity region $1.5 < |y^Z| < 2.5$ at $\sqrt{s} = 13$ TeV. The predictions are made with the SHERPA generator using the CT14NNLO PDF with different values of the IC contribution that correspond to BHPS1 and BHPS2 fits and without IC (no IC). The uncertainty bands represent the uncertainties in the QCD scale (shown only for no IC predictions).

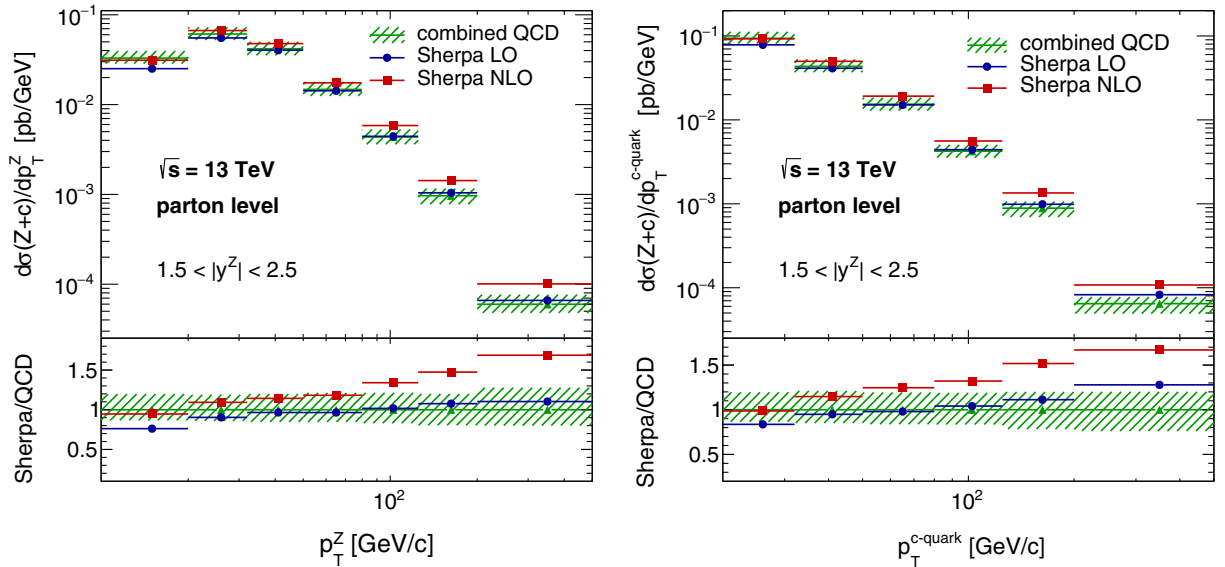


FIG. 5. Parton-level predictions for the production cross section of a Z boson with a c quark as a function of the Z boson (left) and c -quark (right) transverse momenta in the forward rapidity region $1.5 < |y^Z| < 2.5$ at $\sqrt{s} = 13$ TeV. The predictions are made by combined QCD calculations and the SHERPA generator using LO and NLO matrix elements. The CTEQ66 PDF set without any intrinsic charm contribution is used. The uncertainty bands represent the uncertainties in the QCD scale (shown only for combined QCD predictions).

illustrated in Fig. 6. These ratios are calculated using CTEQ66(C) PDF sets with no IC and BHPS2 fit. One can see that including parton showers does significantly decrease the excess in the spectrum caused by the nonzero IC component, while adopting the ME+PS@NLO instead of the ME+PS@LO approach makes little difference. Thus,

both SHERPA predictions made at a particle level give the IC effect in the forward region at $200 < p_T < 500$ GeV (irrespective of whether p_T of the jet or of the Z boson is considered) of the order of 10%–20%, compared to the much larger effect predicted by the parton-level calculations (SHERPA at LO or the combined QCD approach) to be at the

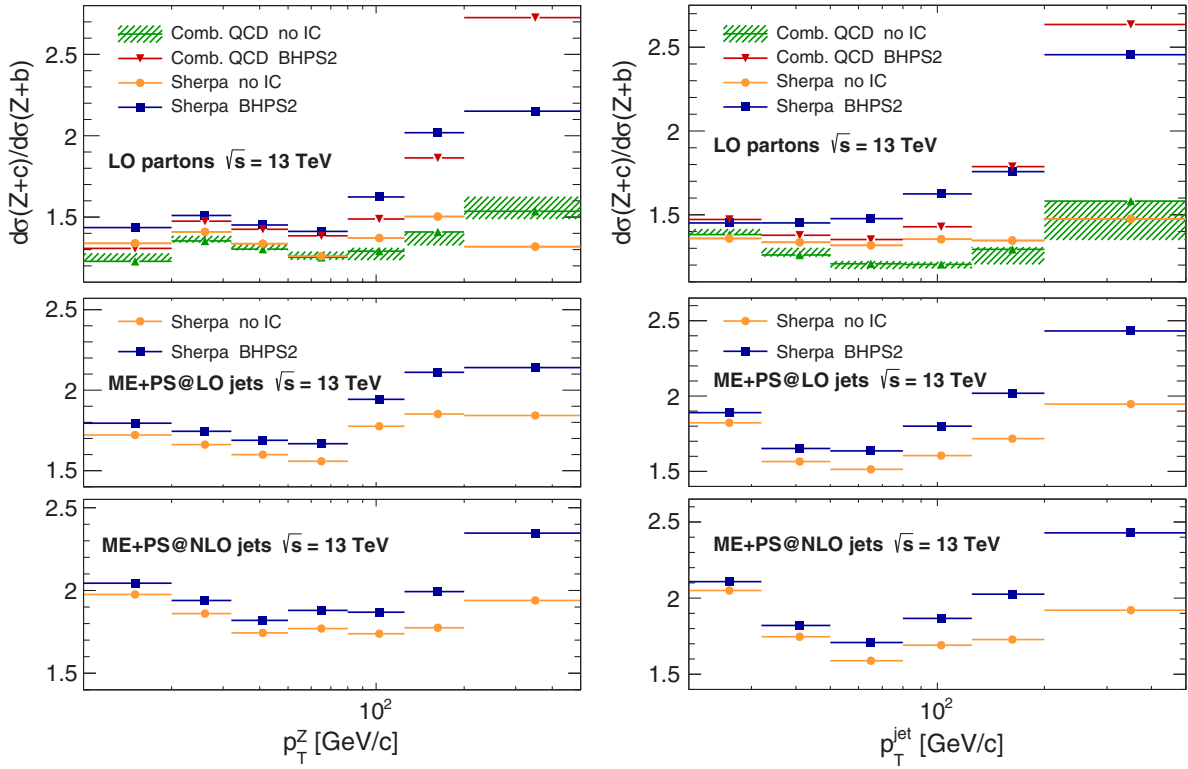


FIG. 6. Predictions for the ratio of the production cross sections of the $Z + c$ jet and of $Z + b$ jet as a function of the Z boson (left) and HF-jet (right) transverse momenta in the forward rapidity region $1.5 < |y^Z| < 2.5$ at $\sqrt{s} = 13$ TeV. The predictions are made with the SHERPA generator at the parton level using the LO matrix element (top panels) and at the particle level using the ME+PS@LO (middle panels) and ME+PS@NLO (bottom panels) models. Predictions of the combined QCD are also shown in the top panel. CTEQ66(C) PDF sets with no IC and BHPS2 fit are used.

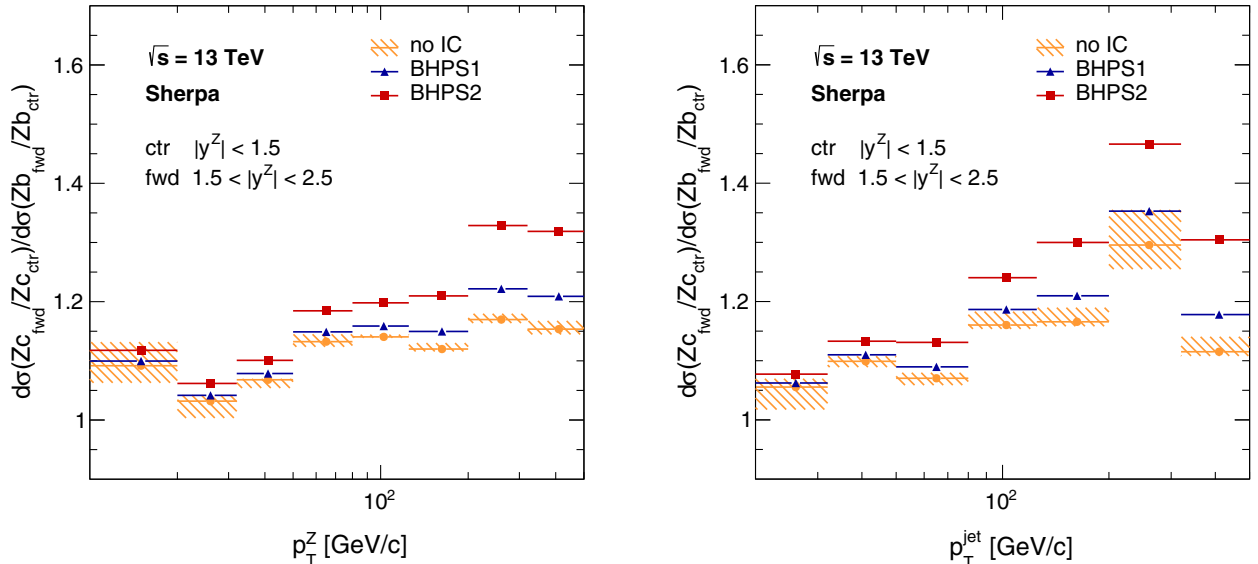


FIG. 7. Predictions for the double ratio as a function of the Z boson (left) and HF-jet (right) transverse momenta at $\sqrt{s} = 13$ TeV. The double ratio is the ratio of the $Z + c$ -jet production cross section in the forward region $1.5 < |y^Z| < 2.5$ to the cross section in the central region $|y^Z| < 1.5$, divided by the same ratio for $Z + b$ -jet production. The predictions are made with the SHERPA generator using the CT14NNLO PDF with different values of the IC contribution that correspond to BHPS1 and BHPS2 fits and without IC (no IC). The uncertainty bands represent the uncertainties in the QCD scale (shown only for no IC predictions).

level of a factor of about 2. This observation is in qualitative agreement with that made in Ref. [12] when comparing the predictions for integral cross sections of $Z + c$ -jet production from fixed-order MCFM calculations and those from SHERPA within the ME+PS@LO approach.

Now, we turn to the discussion of our theoretical uncertainties and uncertainties of the LHC measurements. These uncertainties have been shown [13] to impose a strong restriction on the precision of the IC probability estimation from the experimental data. So, new observ-

- [5] M. Franz, M. V. Polyakov, and K. Goeke, Heavy quark mass expansion and intrinsic charm in light hadrons, *Phys. Rev. D* **62**, 074024 (2000).
- [6] V. A. Bednyakov, M. A. Demichev, G. I. Lykasov, T. Stavreva, and M. Stockton, Searching for intrinsic charm in the proton at the LHC, *Phys. Lett. B* **728**, 602 (2014).
- [7] P.-H. Beauchemin, V. A. Bednyakov, G. I. Lykasov, and Y. Y. Stepanenko, Search for intrinsic charm in vector boson production accompanied by heavy flavor jets, *Phys. Rev. D* **92**, 034014 (2015).
- [8] A. V. Lipatov, G. I. Lykasov, Y. Y. Stepanenko, and V. A. Bednyakov, Probing proton intrinsic charm in photon or Z boson production accompanied by heavy jets at the LHC, *Phys. Rev. D* **94**, 053011 (2016).
- [9] R. D. Ball, V. Bertone, M. Bonvini, S. Carrazza, S. Forte, A. Guffanti, N. P. Hartland, J. Rojo, and L. Rottoli (NNPDF Collaboration), A determination of the charm content of the proton, *Eur. Phys. J. C* **76**, 647 (2016).
- [10] S. J. Brodsky and S. Gardner, Comment on New Limits on Intrinsic Charm in the Nucleon from Global Analysis of Parton Distributions, *Phys. Rev. Lett.* **116**, 019101 (2016).
- [11] P. Jimenez-Delgado, T. J. Hobbs, J. T. Londergan, and W. Melnitchouk, New Limits on Intrinsic Charm in the Nucleon from Global Analysis of Parton Distributions, *Phys. Rev. Lett.* **114**, 082002 (2015).
- [12] T.-J. Hou, S. Dulat, J. Gao, M. Guzzi, J. Huston, P. Nadolsky, C. Schmidt, J. Winter, K. Xie, and C. P. Yuan, CT14 intrinsic charm parton distribution functions from CTEQ-TEA global analysis, *J. High Energy Phys.* **02** (2018) 059.
- [13] V. A. Bednyakov, S. J. Brodsky, A. V. Lipatov, G. I. Lykasov, M. A. Malyshev, J. Smiesko, and S. Tokar, Constraints on the intrinsic charm content of the proton from recent ATLAS data, [arXiv:1712.09096](https://arxiv.org/abs/1712.09096).
- [14] M. Aaboud *et al.* (ATLAS Collaboration), Measurement of differential cross sections of isolated-photon plus heavy-flavour jet production in pp collisions at $\sqrt{s} = 8$ TeV using the ATLAS detector, *Phys. Lett. B* **776**, 295 (2018).
- [15] J. M. Campbell and R. Keith Ellis, Next-to-leading order corrections to $W + 2$ jet and $Z + 2$ jet production at hadron colliders, *Phys. Rev. D* **65**, 113007 (2002).
- [16] E. M. Levin, M. G. Ryskin, Yu. M. Shabelski, and A. G. Shuvaev, Heavy quark production in semihard nucleon interactions, *Yad. Fiz.* **53**, 1059 (1991) [*Sov. J. Nucl. Phys.* **53**, 657 (1991)].
- [17] S. Catani, M. Ciafaloni, and F. Hautmann, High-energy factorization and small x heavy flavor production, *Nucl. Phys.* **B366**, 135 (1991).
- [18] J. C. Collins and R. Keith Ellis, Heavy quark production in very high-energy hadron collisions, *Nucl. Phys.* **B360**, 3 (1991).
- [19] T. Gleisberg, S. Hoeche, F. Krauss, M. Schonherr, S. Schumann, F. Siegert, and J. Winter, Event generation with SHERPA 1.1, *J. High Energy Phys.* **02** (2009) 007.
- [20] S. P. Baranov, H. Jung, A. V. Lipatov, and M. A. Malyshev, Associated production of Z bosons and b-jets at the LHC in the combined k_T + collinear QCD factorization approach, *Eur. Phys. J. C* **77**, 772 (2017).
- [21] G. Aad *et al.* (ATLAS Collaboration), Measurement of differential production cross-sections for a Z boson in association with b-jets in 7 TeV proton-proton collisions with the ATLAS detector, *J. High Energy Phys.* **10** (2014) 141.
- [22] A. M. Sirunyan *et al.* (CMS Collaboration), Measurement of associated Z + charm production in proton-proton collisions at $\sqrt{s} = 8$ TeV, *Eur. Phys. J. C* **78**, 287 (2018).
- [23] B. Andersson *et al.* (Small x Collaboration), Small x phenomenology: Summary and status, *Eur. Phys. J. C* **25**, 77 (2002).
- [24] J. R. Andersen *et al.* (Small x Collaboration), Small x phenomenology: Summary and status, *Eur. Phys. J. C* **35**, 67 (2004).
- [25] J. R. Andersen *et al.* (Small x Collaboration), Small x Phenomenology: Summary of the 3rd Lund Small x Workshop in 2004, *Eur. Phys. J. C* **48**, 53 (2006).
- [26] M. Ciafaloni, Coherence effects in initial jets at small Q^2/s , *Nucl. Phys.* **B296**, 49 (1988).
- [27] S. Catani, F. Fiorani, and G. Marchesini, QCD coherence in initial state radiation, *Phys. Lett. B* **234**, 339 (1990).
- [28] S. Catani, F. Fiorani, and G. Marchesini, Small x behavior of initial state radiation in perturbative QCD, *Nucl. Phys.* **B336**, 18 (1990).
- [29] F. Hautmann and H. Jung, Transverse momentum dependent gluon density from DIS precision data, *Nucl. Phys.* **B883**, 1 (2014).
- [30] F. Krauss, R. Kuhn, and G. Soff, AMEGIC++ 1.0: A matrix element generator in C++, *J. High Energy Phys.* **02** (2002) 044.
- [31] T. Gleisberg and S. Hoeche, Comix, a new matrix element generator, *J. High Energy Phys.* **12** (2008) 039.
- [32] F. Cascioli, P. Maierhofer, and S. Pozzorini, Scattering Amplitudes with Open Loops, *Phys. Rev. Lett.* **108**, 111601 (2012).
- [33] S. Schumann and F. Krauss, A parton shower algorithm based on Catani-Seymour dipole factorisation, *J. High Energy Phys.* **03** (2008) 038.
- [34] S. Hoeche, F. Krauss, M. Schonherr, and F. Siegert, QCD matrix elements + parton showers: The NLO case, *J. High Energy Phys.* **04** (2013) 027.
- [35] S. Hoeche, F. Krauss, S. Schumann, and F. Siegert, QCD matrix elements and truncated showers, *J. High Energy Phys.* **05** (2009) 053.
- [36] P. M. Nadolsky, H.-L. Lai, Q.-H. Cao, J. Huston, J. Pumplin, D. Stump, W.-K. Tung, and C. P. Yuan, Implications of CTEQ global analysis for collider observables, *Phys. Rev. D* **78**, 013004 (2008).
- [37] F. Krauss, D. Napoletano, and S. Schumann, Simulating b-associated production of Z and Higgs bosons with the SHERPA event generator, *Phys. Rev. D* **95**, 036012 (2017).
- [38] S. J. Brodsky, M. Mojaza, and X.-G. Wu, Systematic scale-setting to all orders: The principle of maximum conformality and commensurate scale relations, *Phys. Rev. D* **89**, 014027 (2014).